Storm surges along the Western coast of Norway

By B. GJEVIK, *Institute of Geophysics, University of Oslo* and L. P. RØED, *Institute of Mathematics, University of Oslo, Norway*

(Manuscript received November 8, 1974; in final form March 13, 1975)

ABSTRACT

Storm surge situations along the western coast of Norway between 62° N and 68° N are examined. The observations show that large storm surges are caused by strong south westerly winds acting along a large section of the coast. This situation occurs when an intense low pressure center moves relatively close to the coast and in a direction nearly parallel to it. A model of surge generation by propagating wind fields acting along a straight coast is studied. Analytical solutions for the surge amplitude along the coast are obtained and discussed. The theory is applied to storm surge situations along the western coast of Norway, and it shows that the wind stress in the direction along the coast and the Coriolis force are important forces for the generation of large surges. The wind stress component normal to the coast (i.e. north westerly winds) and the changes in the atmospheric pressure contribute less to the surge.

1. Introduction

The effect of wind and atmospheric pressure on the sea level has been observed and studied for ages in order to be able to foresee the occurrence of catastrophic surges. References to the efforts in this field in various regions of the world is given in the survey articles by Welander (1961) and Bretschneider (1967).

Also along the coasts of Norway storm surges occasionally cause extensive damage to coastal constructions and ships, and some time even the death of people. Tales of catastrophic surges at Grip, a small island on the western coast of Norway, are reported by Helland (1911). About 1650 most of the population of the island of Grip (at that time about 50 people) were killed during a storm associated by an exceptional storm surge. Also in 1797 a storm surge swept the island. This time the inhabitants took refuge in the church which was situated at the highest point on the island, which is approximately 10 m above the sea level. Some people were, however, killed, and the damage to piers and houses were severe.

Catastrophic surges have also occurred at Ona, another low island on the western coast of Norway. In the spring of 1670, 48 of a population of 50 people are reported to be killed during a storm which obviously has flooded the island (Stiftsboken for Nidaros bispedømme, 20 August 1749).

It is well known that along the western coast of Norway, between 62° N and 66° N, extreme surge conditions usually occur during south westerly winds, i.e. with wind direction parallel to the coast. Severe damage occurs, however, only if the storm generates high seas. This situation usually happens if the south westerly wind shifts to a strong westerly wind before the amplitude of the surge has decayed.

Except for a study by Johansen (1959) of surges along the south eastern coast of Norway, little has been done to analyse extreme surge conditions and to develop methods of forecasting damaging events in these waters. In this study we will examine in detail some storm surge conditions along a section of the western coast of Norway, from 62° N to 68° N, and based on some very simplified models of wind generated surges, we shall propose methods of forecasting surges in these regions.

The generation of large storm surges is a complicated phenomenon which is caused both by the drag on the sea exerted by the wind, and by the changes in atmospheric pressure. The surge might also be amplified by the topography of the coast line. Hence storm surges at a cer-

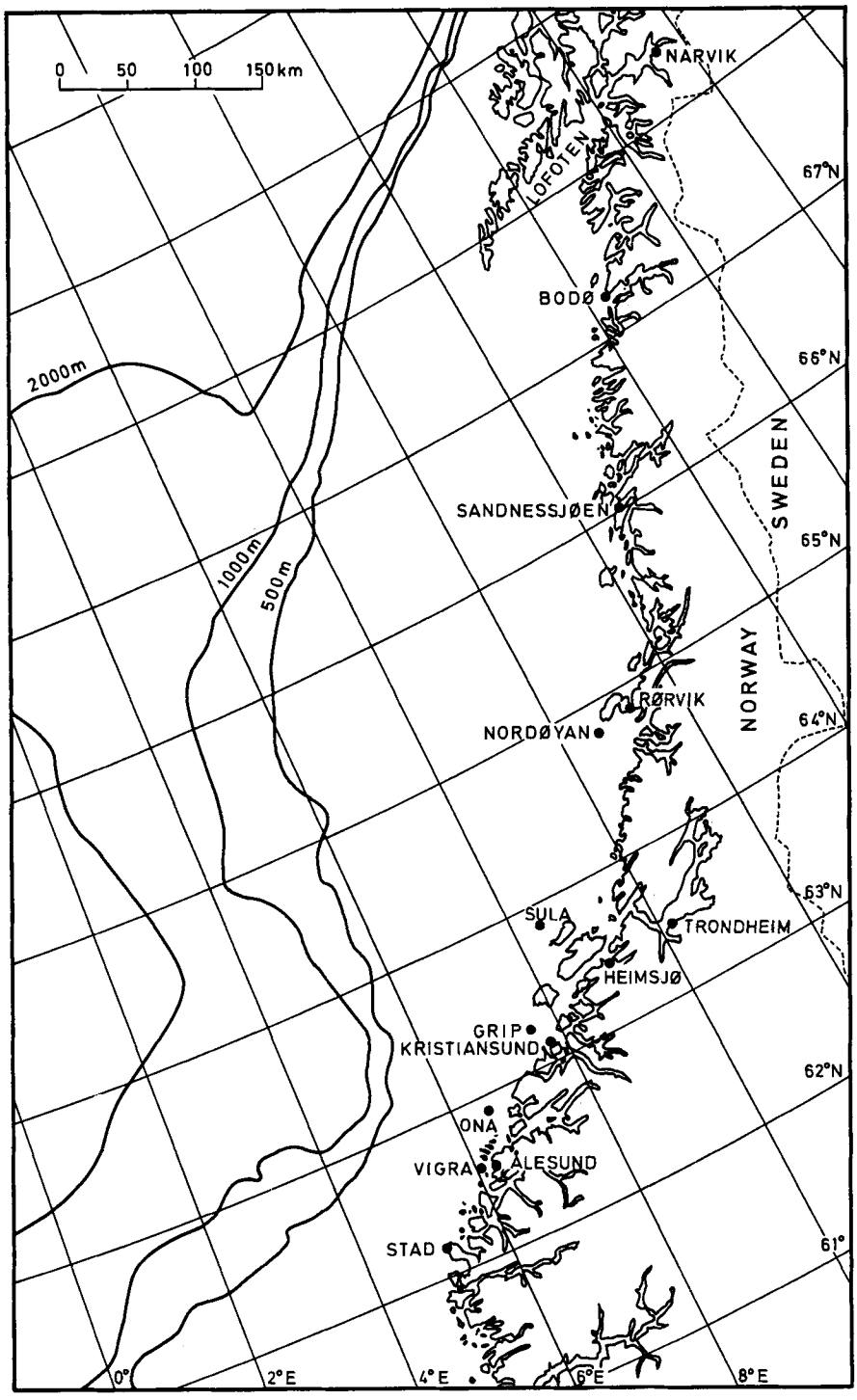

Fig. 1. Map of the Norwegian coast with depth contours in meters.

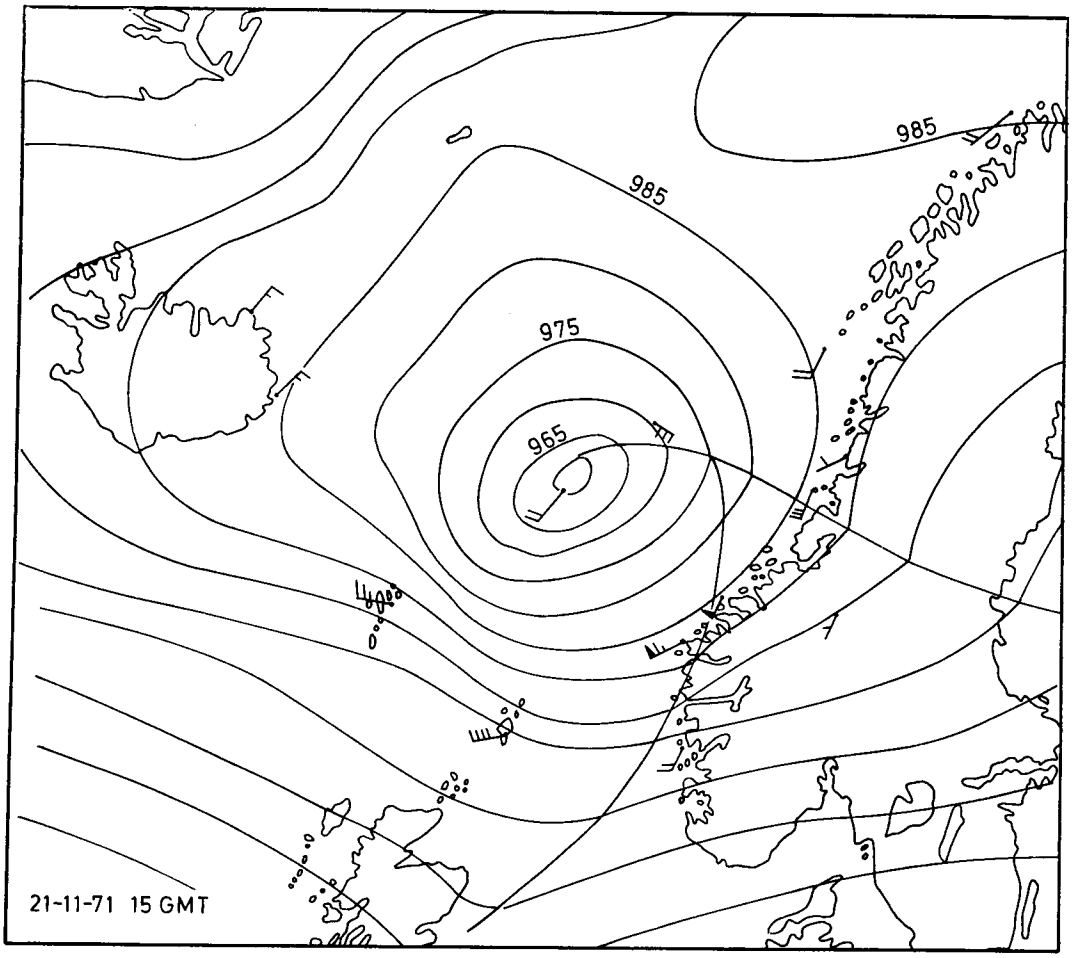

Fig. 2a. Weather map from 2-11-1971, 15 GMT.

tain location might be generated under different meteorological conditions.

During special astronomical situations the moon and the sun attain their minimum distance from the Earth. When this happens the tidal forces become considerably larger than usual, and therefore cause a large tide. It is evidenced that catastrophic surges along the western coast of Norway most often occur during such astronomical situations (E. Jensen, private communication, 1973). Special meteorological conditions are, however, required for the generation of large surges in these regions. If a wind or pressure generated surge coinside with a high tide, this will lead to catastrophic situations.

In this study of storm surges along the coast of Norway between 62° N and 68° N we shall explore how a special meteorological situation with intense south westerly winds along the coast causes large storm surges in this region. Generation of large storm surges in this region under meteorological conditions different from those examined here, is, however, unlikely. This conjecture is supported both by the observation and by the theoretical studies in section 3. In section 2 we present observations of three storm surges along the western coast of Norway. These observations indicate that for storm surges along the coast from Stad to Bodø, the main part of the surge can be attributed to the drag on the sea caused by the wind. In section

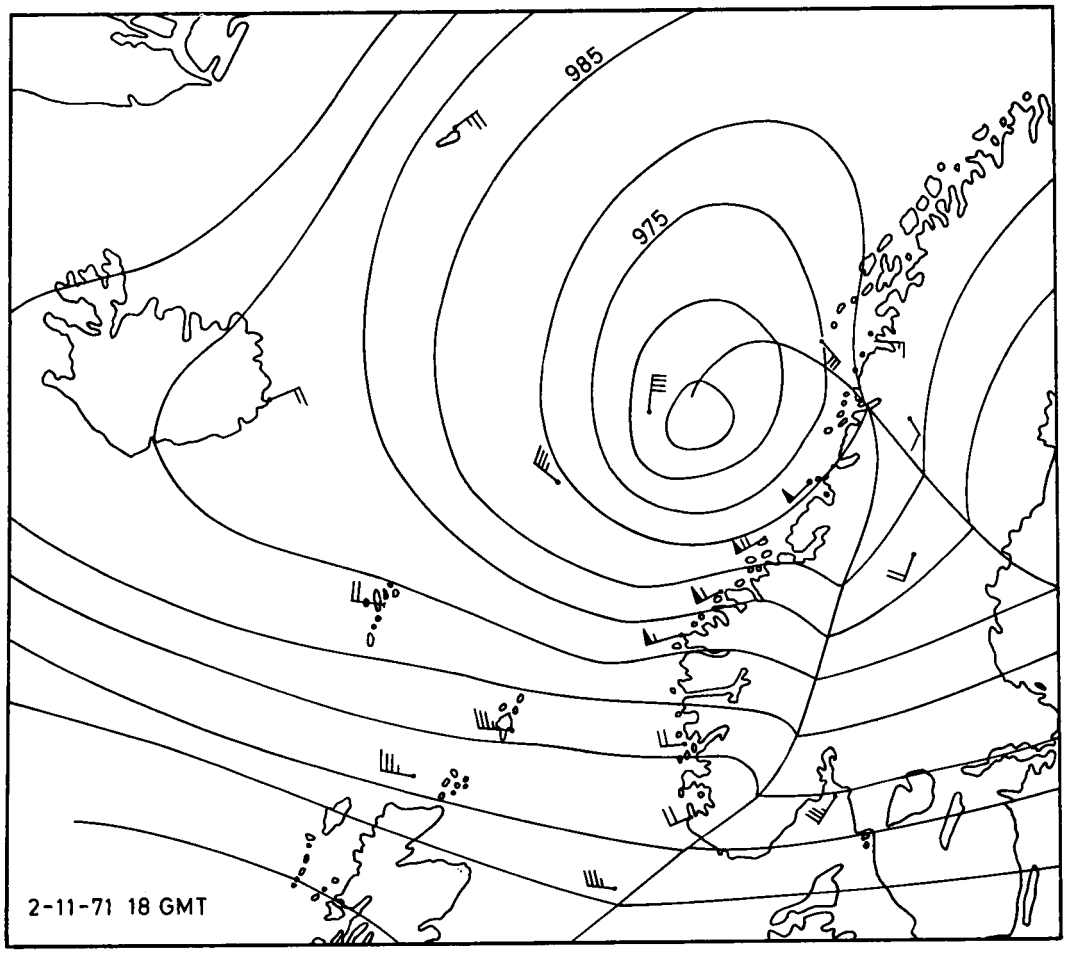

Fig. 2b. Weather map from 2-11-1971, 18 GMT.

3 we therefore study analytically the surge generation by a wind field moving along a straight coast. In section 4 these theoretical studies are compared with the observations and possible methods of forecasting surges are discussed. A map of the western coast of Norway, which includes most of the geographical names referred to in the text, is given in Fig. 1.

2. Observation of storm surges along the western coast of Norway

Of numerous cases with storm surges along the western coast of Norway, we shall examine three cases in details. The first case occurred on the 2nd of November 1971 and the second and third cases, respectively, on the 30th and 31st of December 1972. Subsequently we refer to these cases by Cases I, II, and III. Case I is exceptional with surge amplitudes higher than 1 m. Since the peak of the storm surge nearly coinsided with spring tide along the coast between Sula and Sandnessjøen, the sea level in this region rose to the highest level recorded in this century. Cases II and III are believed to represent more normal situations which frequently occur.

A sequence of surface weather maps from the 2nd of November 1971 are shown in Figs. 2*a*, *b*, and *c*. A low pressure system with center pressure at about 965 millibar moves in a north

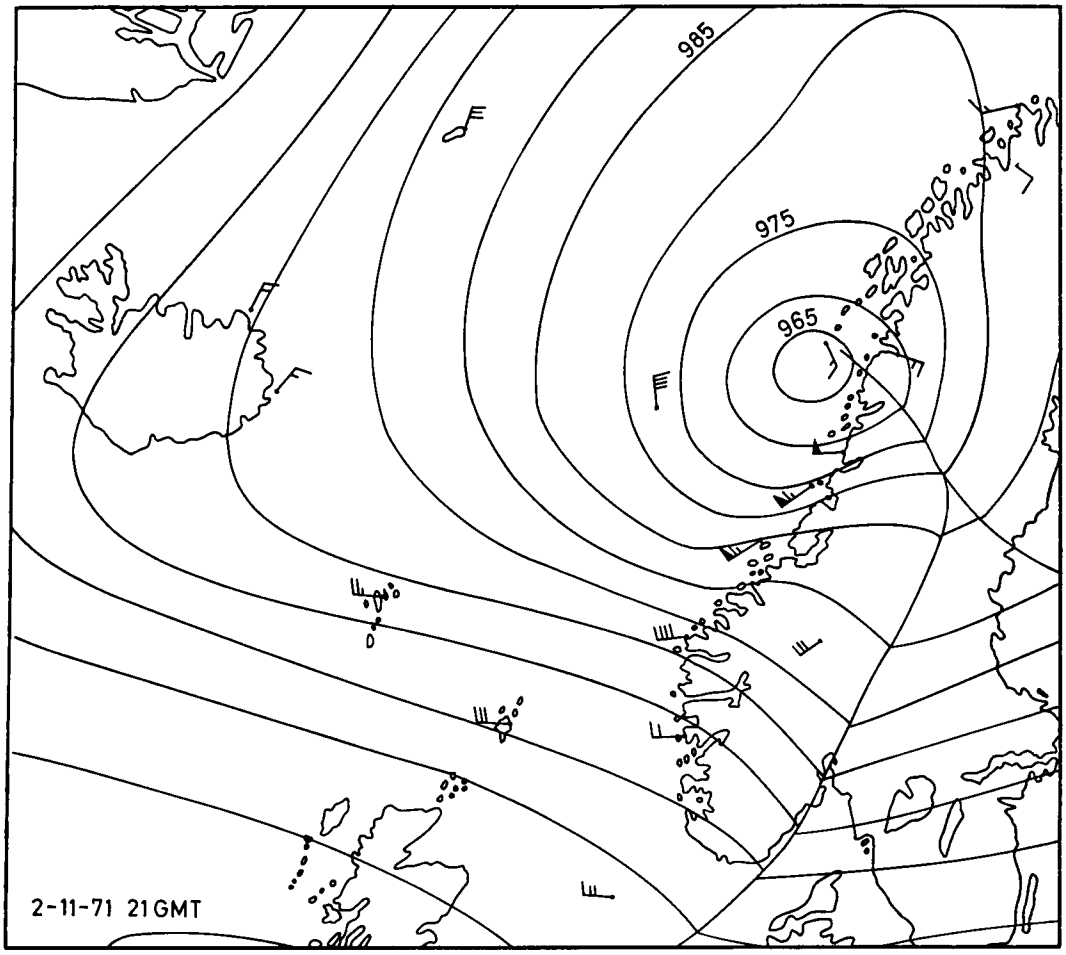

Fig. 2c. Weather map from 2-11-1971, 21 GMT.

easterly direction in the Norwegian sea and crosses the coast line at Lofoten. The low pressure system creates an intense south westerly wind field propagating along the coast. The recordings of the wind speed (averaged over 10 min intervals) at three recording stations are displayed in Fig. 3. These observations show that the wind speeds, particularly along the section of the coast between 63° N and 65° N, are exceptionally high exceeding 35 m/s (or 70 knots) at Nordøyan. A plot of amplitude verses time for the surge is obtained from the tidal records at Kristiansund, Rørvik and Narvik. The predicted sea level (based on tidal tables published by Norges Sjøkartverk, Stavanger, Norway) is subtracted from the recorded sea level and the residual, which is assumed to represent the amplitude of the storm surge, is displayed in Fig. 4. These observations show that the storm surge is felt over a large area and that the maximum surge amplitude occurred between 64° N and 66° N. In addition to the recorded surge amplitudes displayed in Fig. 4, we have also estimated the maximum surge amplitude at a few other places along the coast. The results are given in Table 1.

Since both Hammerfest (70.7° N, 23.7° E) and Tromsö (69.7° N, 19.5° E) are situated north of the wind field, the surge at these two places is most likely generated by the changes in the atmospheric pressure when the center of the low pressure system moves eastward over

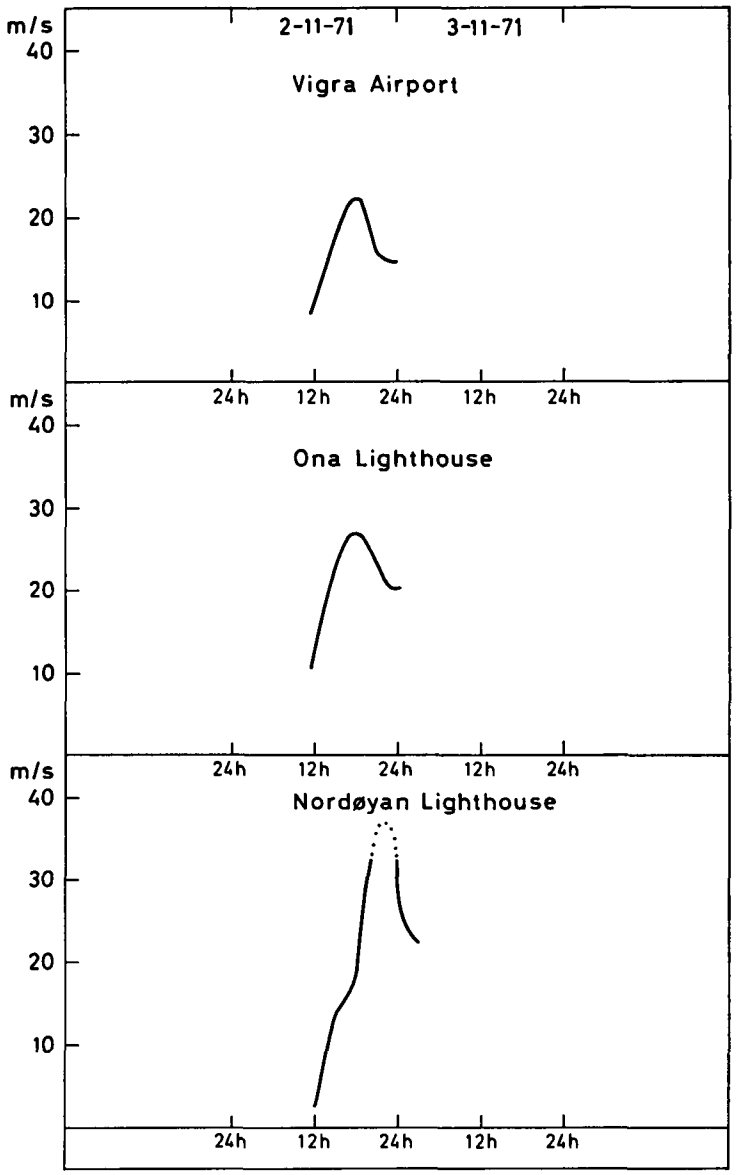

Fig. 3. Wind speed averaged over 10 min intervals.

the Lofoten region. A free wave transmitted northward along the coast from regions with high surge amplitudes, might also contribute to the surge at Tromsö and Hammerfest.

The observations for Cases II and III are presented in the same way as for Case I. Weather maps from the 30th and 31st of December 1972, are presented in Figs. 5 and 6, respectively, and the recordings of wind speeds and surge amplitudes are displayed in Figs. 7 and 8. On the 30th of December a low pressure system with center pressure about 955 millibar situated in the Norwegian sea, far west of the Norwegian coast, is moving slowly in a north easterly direction. The low pressure system creates south westerly winds along the western

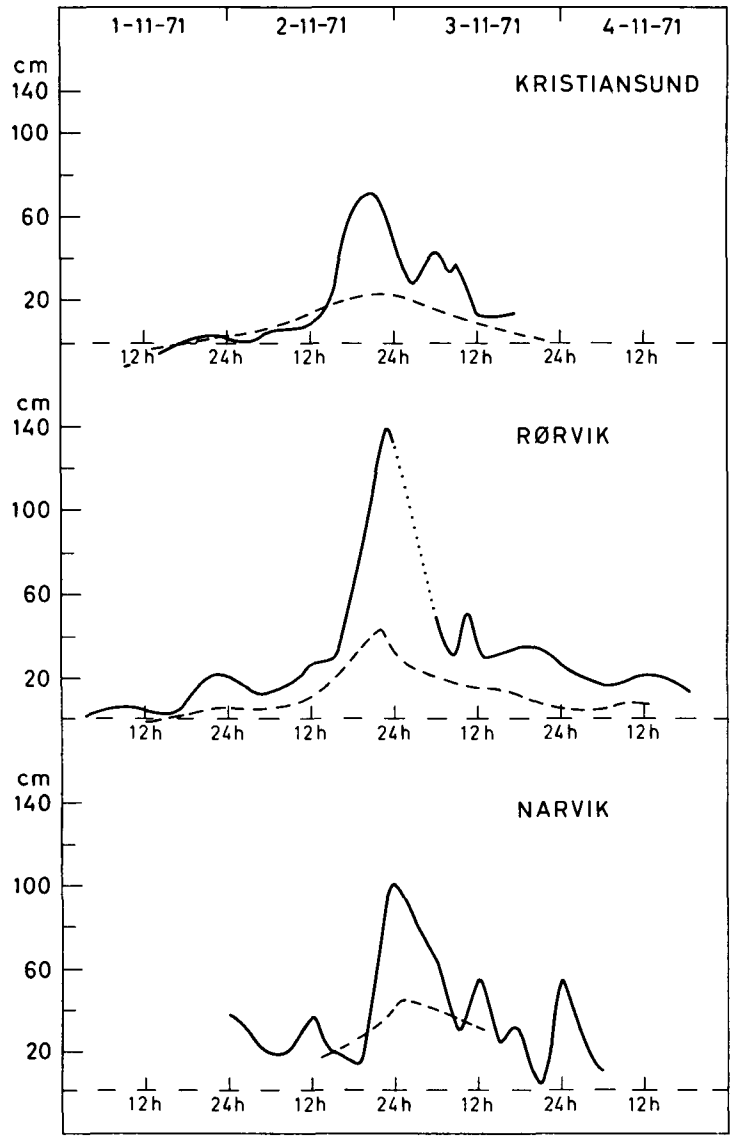

Fig. 4. Surge amplitudes (solid lines). Observations missing (dotted lines). The estimated effect of atmospheric pressure on the sea level (broken lines).

coast of Norway. The wind field in this case extends far off the coast and along the entire region of the coast from Stad to Lofoten.

On the 31st of December a low pressure system in the Norwegian sea with center pressure about 975 millibar, creates an intense south westerly wind field along the coast of Norway. The path of the low pressure system in this case is similar to that in Case I. Since the center of the low pressure system is moving relatively

Table 1

	Estimated maximum surge amplitude (cm)
Ålesund	40
Heimsjö	75
Trondheim	100
Sandnessjöen	120
Hammerfest	40
Tromsö	50

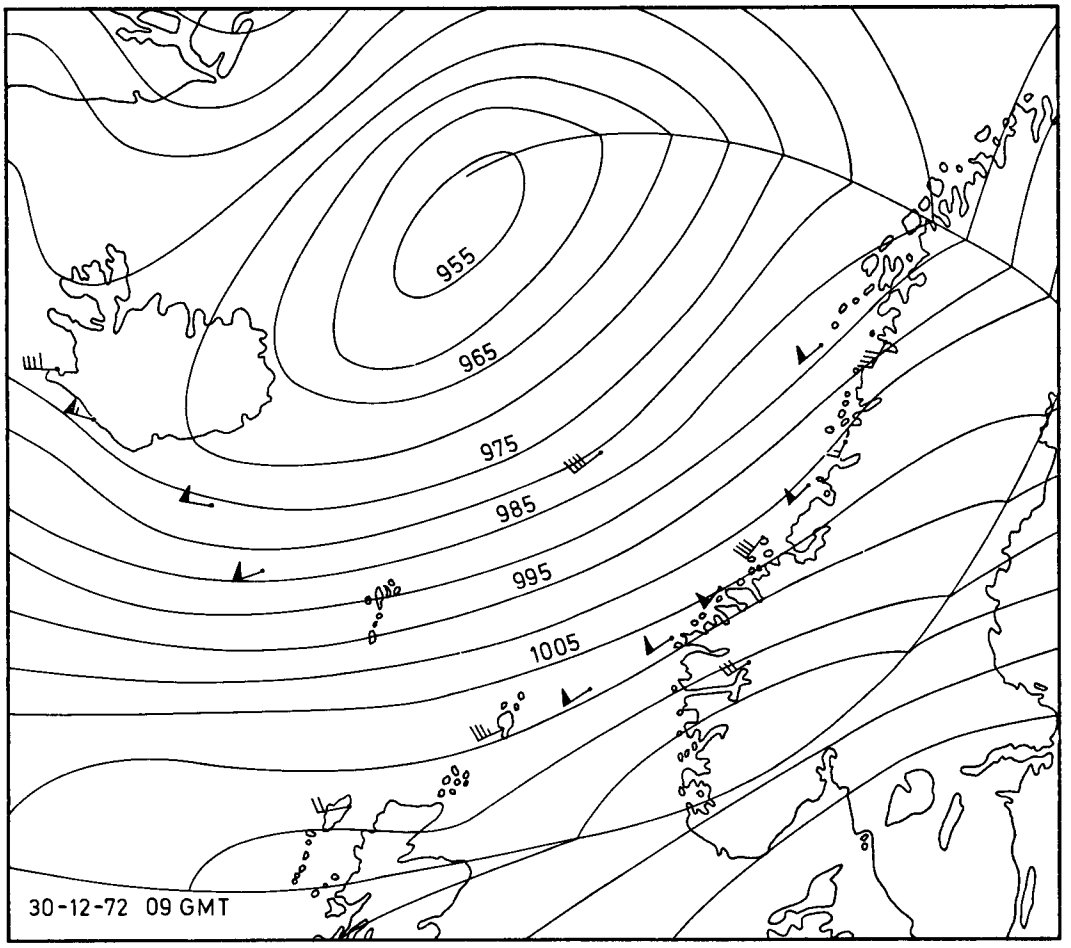

Fig. 5. Weather map from 30-12-1972, 09 GMT.

close to the Norwegian coast, the south westerly wind field is confined to the continental shelf. In that respect, Case I and Case III are similar although the wind speeds (and the recorded surge amplitudes) particularly north of 63° N are considerably larger in Case I than in Case III. At Narvik, however, the surge amplitude is larger in Case III than in Case I. Since the low pressure systems both in Case I and Case III cross the coast line at Lofoten, the surges at Narvik might be severely influenced by the changes in atmospheric pressure and also by the topography of the coast and the continental shelf.

The most striking feature of Cases I and III is the strong winds with a direction almost parallel to the coast. Another feature is the propagation of these wind fields from Stad to 67° N. From the observations we find that the peak of the wind fields moves with an average velocity of about 25 m/s. In Case II the cold front associated with the low pressure system moves almost normal to the coast and the south westerly wind field is felt almost at the same time along the entire section of the coast between 62° N and 68° N. The records of the surges in Figs. 4 and 8 reveal that there is a remarked time lag between the peak surge at Kristiansund, Rörvik and Narvik in Cases I and III. In Case II the time lag is negligible. We have also in a few other cases examined the observations of recorded surges along the re-

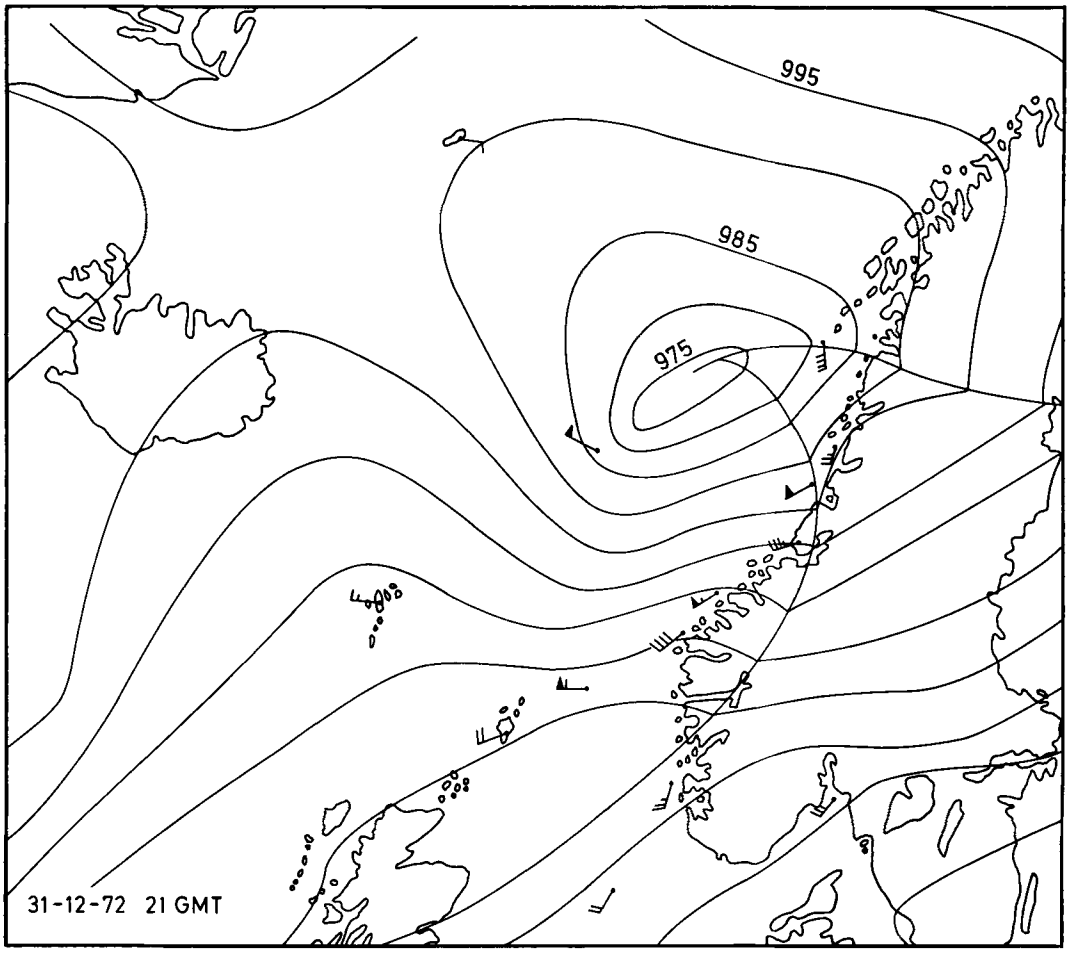

Fig. 6. Weather map from 31-12-1972, 21 GMT.

gion of the western coast of Norway between 62° N to 68° N. Also in these cases we have found that intense south westerly wind fields, which propagate along the coast, generate surges with amplitude depending on the wind speed and the extension of the wind field.

The changes in atmospheric pressure, will certainly effect the sea level. We have estimated this effect by considering the static effect of the horizontal atmospheric pressure gradients. The difference between the actual barometric pressure and the mean seasonal pressure is obtained and converted to the equivalent change in sea level. A change in pressure of 1 millibar corresponds approximately to a change in sea level of 1 cm. The static effect of the atmospheric pressure on sea level is then plotted (by broken lines) in Figs. 4 and 8. These diagrams show that the atmospheric pressure has some effect on the surge amplitude in Case I, but a negligible effect in Cases II and III. These estimates are correct only if the pressure variations are sufficiently slow. The time variation of the pressure field might become important particularly in shallow water and thus invalidating our estimates. This may be true for the surge recorded at Narvik in Cases I and III.

The observations indicate, however, that the wind drag is the most important factor for surge generation between Stad and Bodö. On

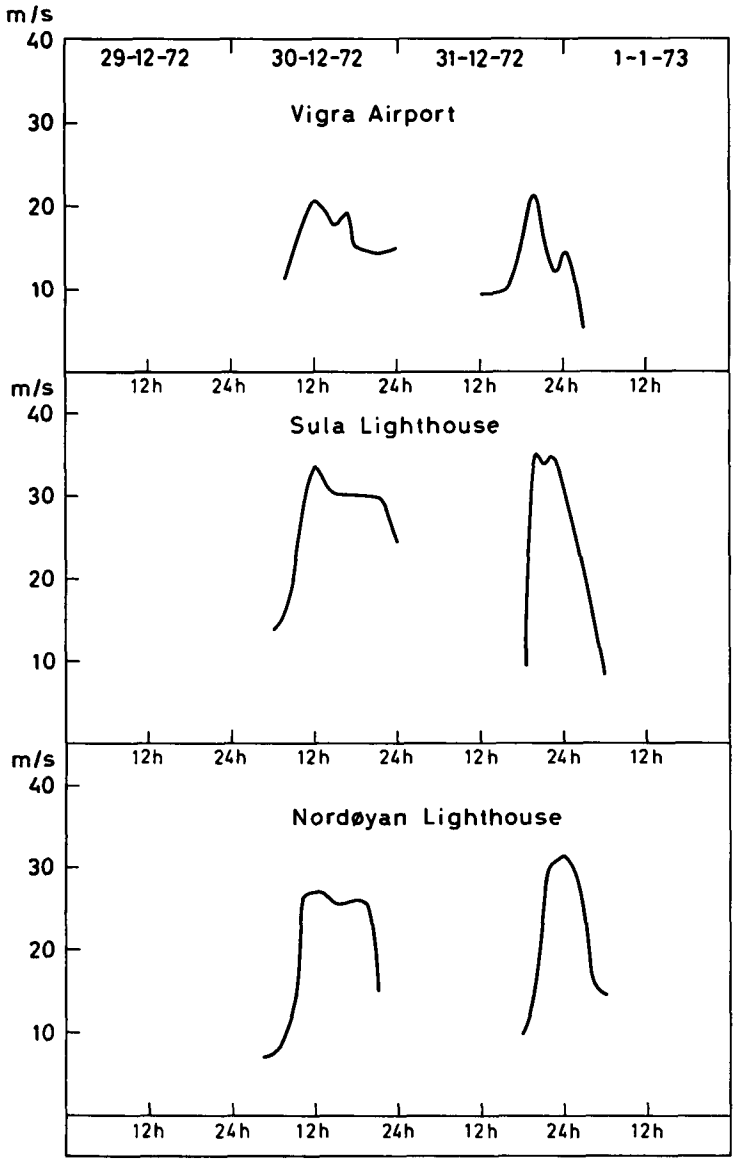

Fig. 7. Wind speed averaged over 10 min intervals.

basis of this conjecture we shall in the next section propose a model for wind generated surges in this region.

3. Theory

We shall consider a homogeneous incompressible fluid with density ϱ and we shall describe the motion of this fluid relative to a cartesian coordinate system (x, y, z) with the z-axis pointing upward in the vertical direction. The fluid is bounded by a bottom surface $z = -H(x, y)$ where H is a function of the horizontal coordinates x and y. The surface of the fluid is at $z = \eta(x, y, t)$ where η is a function of x and y and of time (t). In the undisturbed state the

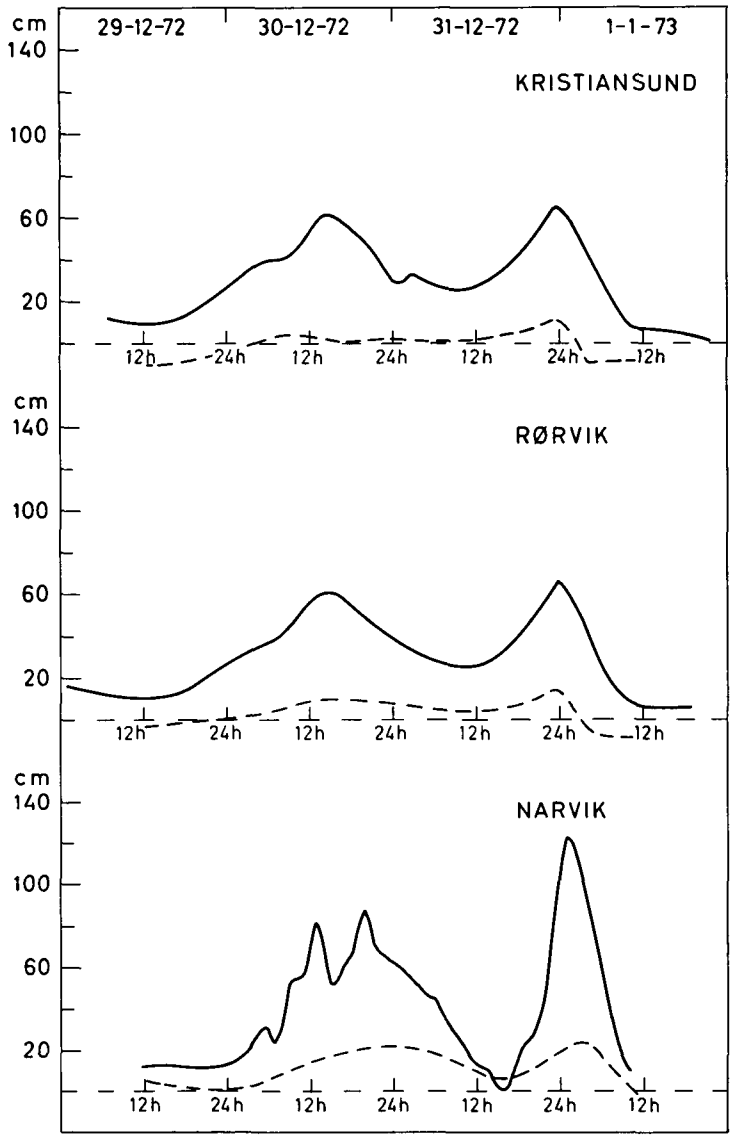

Fig. 8. Surge amplitudes (solid lines). The estimated effect of atmospheric pressure on the sea level (broken lines).

fluid is at rest and the surface is the plane $z = 0$.

We shall consider the response of the fluid to pressure and wind systems of large horizontal extent compared to the depth. Hence we are justified in making the hydrostatic approximations in the equations of motion. We shall also assume that the surface displacement, its slope, and the velocity field generated by wind and pressure are sufficiently small so that the equation of motion can be linearized with respect to these parameters. Moreover we shall assume that the dominant stresses introduced in the ocean by the action of the wind are the horizontal components of the shear stresses. We denote the x and y components of shear stresses by τ_x and τ_y respectively. Due to the large horizontal extent of the wind system, the derivatives of τ_x and τ_y with respect to the

Table 2

Wind speed (m/s)	C_D	η_s (cm)
25	2.5×10^{-3}	16
30	3.0×10^{-3}	27
35	3.5×10^{-3}	43

horizontal coordinates will be neglected compared to the derivative with respect to z. If we introduce the horizontal components of volume flux and integrate the equation of motion from the bottom to the surface we find

$$\frac{\partial Q_x}{\partial t} - fQ_y = -gH\frac{\partial \eta}{\partial x} - \frac{H}{\varrho}\frac{\partial p_0}{\partial x} + \frac{1}{\varrho}\tau_x(z=\eta) - \frac{1}{\varrho}\tau_x(z=-H)$$

$$\frac{\partial Q_y}{\partial t} + fQ_x = -gH\frac{\partial \eta}{\partial y} - \frac{H}{\varrho}\frac{\partial p_0}{\partial y} + \frac{1}{\varrho}\tau_y(z=\eta) - \frac{1}{\varrho}\tau_y(z=-H) \qquad (1)$$

$$\frac{\partial \eta}{\partial t} = -\frac{\partial Q_x}{\partial x} - \frac{\partial Q_y}{\partial y}$$

where Q_x and Q_y is the volume fluxes respectively in the x and y directions. $f = 2\Omega \sin \Phi$ is the Coriolis parameter where Ω is the angular velocity of the Earth and Φ is the latitude (assumed constant in the subsequent analysis).

The shear stresses at the surface and at the bottom may be related respectively to the wind field and the components of volume flux by empirical formulas. The appropriate boundary conditions for eqs. (1) are zero volum flux through the lateral boundaries of the ocean.

The set of eqs. (1) is commonly used for prediction of storm surges. The numerical and analytical solutions to the eqs. (1) for ocean basins of various shapes and for different stress and pressure fields are numerous. For a review of these solutions see Welander (1961), Heaps (1965), and Bretschneider (1967). We have obtained an analytical solution to the eqs. (1) for a moving wind field acting on an ocean of uniform depth and bounded by an infinitely long coast. To our knowledge the solutions to this problem are not previously discussed. Moreover we are able to show that these solutions are relevant for the understanding of the generation of storm surges along the western coast of Norway. We shall assume that either of the components of the surface shear stress can be related to the corresponding wind components by the formula

$$(\tau_x, \tau_y) = \varrho_l C_D (U^2, W^2) \qquad (2)$$

where U and W are the wind components respectively along the x and y-axis, $\varrho_l = 1.2 \times 10^{-3}$ g/cm^3 is the density of the air and C_D is the drag coefficient. To estimate a relevant value of the drag coefficient for the storm situations we shall examine is very difficult. For wind speeds between 5 m/s and 20 m/s a drag coefficient between 10^{-3} and 2×10^{-3} is measured (Phillips, 1966). During strong winds C_D might become considerable larger and a value of C_D up to 3×10^{-3} might be reasonable (Defant, 1961). We therefore assume that C_D varies with the wind speed according to Table 2.

Since the shelf along the western coast of Norway is relatively deep (average depth about 250 m) a bottom current of considerable strength will only develop when the wind drag persist for more than one day (Gammelsrød et al., 1975). The characteristic time duration of the storm surges we shall consider, is less than one day. Accordingly we neglect the effect of the bottom friction and this might be a good approximation up to the final decaying stage of the surge. With no bottom friction, $\tau_x(z=-H) = \tau_y(z=-H) = 0$, and an ocean of uniform depth bounded by a straight coast at $y = 0$, a general solution to eqs. (1) for arbitrary wind and pressure fields and arbitrary initial conditions can be formally obtained by a combined Fourier and Laplace transform technique.

We are mainly interested in discussing the generation of surges by wind field moving along the coast, and we shall for simplicity consider stress and pressure fields of the following form:

$$\tau_x = \varrho T_{0x} F(x,t) e^{-\alpha y}$$
$$\tau_y = \varrho T_{0y} G(x,t) e^{-\beta y} \qquad (3)$$
$$p_0 = \text{constant}$$

for $t \geq 0$. T_{0x}, T_{0y}, α and β are assumed to be constant. F and G are functions of x and t only. The initial conditions are assumed to be

$$Q_x = Q_y = \eta = 0 \qquad (4)$$

and the relevant boundary conditions for finite t are

$$Q_y = 0 \quad \text{for} \quad y = 0$$

$$Q_x \to 0 \quad \text{for} \quad x \to \pm\infty$$

$$Q_y \to 0 \quad \text{for} \quad y \to +\infty \tag{5}$$

We assume that the functions F and G possess a Fourier transform with respect to x

$$(\bar{F}, \bar{G}) = \frac{1}{\sqrt{2\pi}} \int_{-\infty}^{+\infty} (F, G) e^{-ikx} dx \tag{6}$$

where k is a constant and i the imaginary unit, and a Laplace transform with respect to t

$$(\bar{\bar{F}}, \bar{\bar{G}}) = \int_0^{\infty} (F, G) e^{-st} dt \tag{7}$$

where the real part of the constant s is assumed to be positive. The corresponding Fourier and Laplace inversion theorems may be found in text books on the subject (see for example Miles, 1971).

By taking the Fourier and Laplace transform of eq. (1) with the stress and pressure field given by (3) and invoking the initial conditions (4) and the boundary conditions (5), an expression for the transformed surface displacement at $y = 0$ is found

$$\bar{\bar{\eta}}(y=0) = \bar{\bar{\eta}}_1 + \bar{\bar{\eta}}_2 + \bar{\bar{\eta}}_3 \tag{8}$$

where

$$\begin{aligned}
\bar{\bar{\eta}}_1 &= -\frac{ik}{s^2 + c_0^2 k^2} T_{0x} \bar{\bar{F}} \\
\bar{\bar{\eta}}_2 &= \frac{(sf + ik\alpha c_0^2)\left(\sqrt{s^2 + k^2 c_0^2 + f^2} - \alpha c_0\right)}{c_0 (s^2 + k^2 c_0^2)(s^2 + k^2 c_0^2 + f^2 - \alpha^2 c_0^2)} T_{0x} \bar{\bar{F}} \\
\bar{\bar{\eta}}_3 &= -\frac{\left(\sqrt{s^2 + k^2 c_0^2 + f^2} - \beta c_0\right)}{c_0 (s^2 + k^2 c_0^2 + f^2 - \beta^2 c_0^2)} T_{0y} \bar{\bar{G}}
\end{aligned} \tag{9}$$

The velocity $c_0 = \sqrt{gH}$ is the velocity of long gravity waves in absence of rotation. We note that $\bar{\bar{\eta}}_1$ is independent of f and α while $\bar{\bar{\eta}}_3$ represent the effect of the wind stress acting normal to the coast. The derivation of (9) involves only trivial algebra, however lengthy, and the details in the computations will be omitted here. In order to obtain mathematical tractable inversion integrals, the functions F and G have to be chosen properly. On the other hand we require the stress field corresponding to F and G to approximate the stress field acting during storm surge conditions along the western coast of Norway. To meet with both of these requirements we have taken

$$\begin{aligned}
F &= e^{-\varkappa(x - u_0 t)^2} \\
G &= e^{-\varkappa x^2} h(t)
\end{aligned} \tag{10}$$

where $h(t)$ is a function of time, $0 < h(t) \leq 1$. The transformed functions are:

$$\begin{aligned}
\bar{\bar{F}} &= \frac{1}{\sqrt{2\varkappa}} \frac{e^{-k^2/4\varkappa}}{s + iku_0} \\
\bar{\bar{G}} &= \frac{\bar{h}}{\sqrt{2\varkappa}} e^{-k^2/4\varkappa}
\end{aligned} \tag{11}$$

with $\bar{\bar{F}}$ and $\bar{\bar{G}}$ given by (11) the Laplace inversion integral leads to poles at $s = iku_0$ and $s = \pm ikc_0$ in the inversion integrals for η_1 and η_2 and branch points at $s = \pm i\sqrt{f^2 + k^2 c_0^2}$ in the inversion integrals for η_2 and η_3. The inversion procedure is somewhat lengthy but straight forward and only the result needs to be given here. For the surge caused by the wind stress parallel to the coast, we find:

$$\eta_1 = \eta_s \frac{\pi}{2P} \left\{ \frac{1}{1-\nu^2} \operatorname{erf} P(R - \nu\tau) - \frac{1}{2(1+\nu)} \operatorname{erf} P(R + \tau) - \frac{1}{2(1-\nu)} \operatorname{erf} P(R - \tau) \right\} \tag{12}$$

$$\begin{aligned}
\eta_2 = \eta_s \Bigg\{ & \frac{\pi}{2P} \left[\frac{\nu - B}{1-\nu^2} \frac{2}{\pi} \int_0^{\infty} \frac{e^{-\xi^2/4}}{\xi} \frac{\sin \xi P(R - \nu\tau)}{B + \sqrt{1 + \xi^2 P^2 (1-\nu^2)}} d\xi \right. \\
& + \frac{1}{2(1+\nu)} \operatorname{erf} P(R + \tau) \\
& \left. + \frac{1}{2(1-\nu)} \frac{B-1}{B+1} \operatorname{erf} P(R - \tau) \right] \\
& + \frac{2}{\pi} \int_0^{\infty} e^{-\xi^2/4} \int_{\sqrt{1+\xi^2 P^2}}^{\infty} \\
& \times \frac{\sqrt{\chi^2 - (1 + \xi^2 P^2)}\, D(\chi, \xi)}{(\chi^2 - \nu^2 P^2 \xi^2)[\chi^2 + B^2 - (1 + \xi^2 P^2)](\chi^2 - \xi^2 P^2)} \delta\chi\delta\xi \Bigg\}
\end{aligned} \tag{13}$$

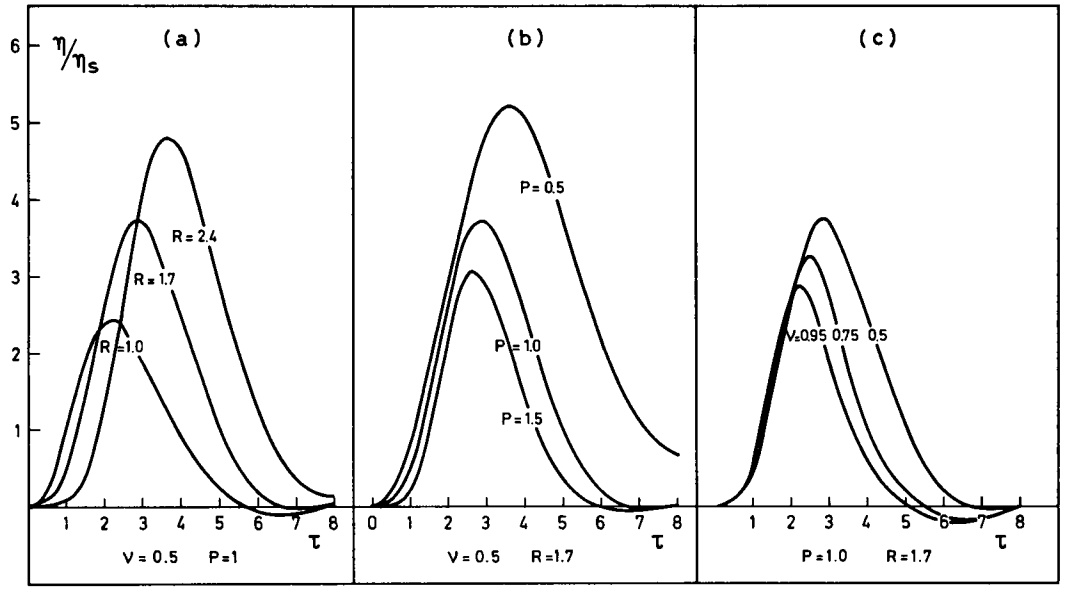

Fig. 9. Theoretical surge amplitudes computed from eqs. (12) and (13) with B = 0. (*a*) $\nu = 0.5, P = 1.0$, and $R = 1.0, 1.7, 2.4$; (*b*) $\nu = 0.5$, $P = 0.5, 1.0, 1.5$, and $R = 1.7$; (*c*) $\nu = 0.5, 0.75, 0.95$, $P = 1.0$, and $R = 1.7$.

where

$$D(\chi, \xi) = (\chi^2 - B\nu^2P^2\xi^2)\cos \xi RP \sin \chi\tau - (\nu - B)P\chi \sin \xi RP \cos \chi\tau$$

and

$$\eta_s = \frac{T_{0x}}{\sqrt{\pi}\, c_0 f}$$

and the dimensionless parameters are defined by

$$\nu = \frac{1}{c_0}u_0, \quad B = \frac{c_0}{f}\alpha, \quad P = \frac{c_0}{f}\sqrt{\varkappa}, \quad R = \frac{f}{c_0}x, \quad \tau = ft \tag{14}$$

In eqs. (12) and (13) we have introduced the error function defined by

$$\operatorname{erf} \phi = \frac{2}{\sqrt{\pi}} \int_0^{\phi} e^{-u^2} du \tag{15}$$

and use have been made of the formula

$$\operatorname{erf} \phi = \frac{2}{\pi} \int_0^{\infty} \frac{e^{-\xi^2/4}}{\xi} \sin(\phi\xi) d\xi \tag{16}$$

(Abramowitz & Stegun, 1964).

For $B = 0$ we have computed the surge amplitude $\eta_{12} = \eta_1 + \eta_2$ as a function of τ (from eqs. (12) and (13)) for different values of the parameters and the results are displayed in Fig. 9. The physical interpretation of the parameters defined by (14) and their effect on the surge amplitude can be summarized as follows: $R = (fx)/c_0$ is a dimensionless measure of the fetch of the wind fields, i.e. the distance between the observation point and the initial position of the wind maximum. Fig. 9*a* demonstrates how the surge amplitude increases with the fetch.

The parameter $P = (c_0\sqrt{\varkappa})/f$ is a Rossby number defined by the characteristic horizontal length scale of the wind field. Small values of P corresponds to wind fields of large extent. As expected we find that the surge amplitude decreases for increasing values of P (Fig. 9*b*).

$B = (\alpha c_0)/f$ is a dimensionless measure of the extent of the wind field perpendicular to the coast. Large values of B characterizes wind fields confined to the coastal regions. We expect that the surge amplitude decreases for increasing values of B and eq. (17) can easily be used to estimate this effect.

$\nu = u_0/c_0$ is a dimensionless measure of the

propagation velocity of the wind field. The dependence of the surge amplitude on ν for values of ν less than unity, is illustrated in Fig. 9c.

For sufficiently small values of P it follows from (13) that the second integral in the expression for η_2 can be neglected and that the denominator in the first integrand can be approximated by $\xi(B+1)$. Invoking (16) we therefore obtain

$$\eta_{12} = \eta_1 + \eta_2 \cong \frac{\eta_s}{B+1} \frac{\pi}{2P} \frac{1}{1-\nu} [\operatorname{erf} P(R-\nu\tau) - \operatorname{erf} P(R-\tau)] \tag{17}$$

Numerical computations show that for values of P up to unity this expression provides the surge amplitude within 10%.

The formula (17) also enables a discussion of the case $\nu \to 1$ and in this case we find

$$\eta_{12} \simeq \frac{\eta_s}{1+B} \sqrt{\pi}\, \tau e^{-P^2(R-\tau)^2}$$

This expression shows that for $R \gg 1/P$ the maximum surge amplitude increases linearly with R. It follows from (17) that for values of $0 < \nu < 1$ ($P \neq 0$), η_{12} is bounded. However, for small values of P, the resonance occurring for $\nu = 1$ is a very slow process which is unimportant for the generation of large surges.

So far we have not discussed the contribution to the surge from the wind stress perpendicular to the coast. For simplicity the expression for $\bar{\eta}_3$ will be inverted only in the case when $(\beta c_0)/f \ll 1$, i.e. the wind field has a large extent in the direction perpendicular to the coast. Invoking (11), we find that in this case

$$\bar{\eta}_3 = \frac{T_{0y}}{\sqrt{2\varkappa c_0}} \frac{e^{-k^2/4\varkappa}\bar{h}}{\sqrt{s^2 + k^2 c_0^2 + f^2}}$$

and by inverting

$$\eta_3 = \eta_s \frac{T_{0y}}{T_{0x}} \int_0^\infty e^{-\xi^2/4} \cos \xi RP \int_0^\tau h(\tau-\chi) J_0 \times [(1+\xi^2 P^2)^{\frac{1}{2}}\chi] d\chi d\xi \tag{18}$$

where J_0 denotes the Bessel function of order zero. Obviously the maximum value of η_3 occurs for $R = 0$. If we take $h(t)$ as a unit step function at $t = 0$, it is easily seen that the maximum value of η_3 is bounded.

The integrals in (18) decrease when P increases and tend to zero for $P \to \infty$. For example when $\tau = 3$ the integrals have the values 2.46 for $P = 0$ and 1.40 for $P = 1$. On the other hand, for some values of the parameters ν, P, and R, the maximum value of η_{12} as function of τ becomes much larger than $(\eta_3)_{\max}$ even when $T_{0y}/T_{0x} \cong 1$ (see Fig. 9 and the discussion above). We shall subsequently see that this is normally the case for the larger storm surges occurring along the western coast of Norway.

Finally the response of the sea level to a pressure field which is independent of the y-coordinate and which is moving along the coast can easily be obtained from the solutions above. For a pressure field

$$p(x, t) = p_0 - \Delta p_0 e^{-\varkappa(x-u_0 t)^2} \tag{19}$$

where p_0 is the mean atmospheric pressure at sea level, and Δp_0 is the maximum pressure deviation from the mean value, the surge at the coast is simply found by differentiating the solutions in (12) and (13) with respect to x putting $B = 0$ and substituting $\eta_s = \Delta p_0/\varrho g$. For values of $P \leq 1$ the formula (17) is valid and we find that the sea level variation at the coast due to the pressure field (19) is

$$\eta_p = \frac{\Delta p}{\varrho g} \cdot \frac{1}{1-\nu} [e^{-P^2(R-\nu\tau)^2} - e^{-P^2(R-\tau)^2}] \tag{20}$$

If the pressure field also decreases in the direction perpendicular to the coast (this is the case for the storm surge situations examined in the next section), an analytical treatment becomes more involved. However, in this case we expect the sea level variations due to pressure variation to be somewhat less than in (20).

4. Comparison between theory and observations

The application of the present idealized theory to the problem of surge generation along the western coast of Norway must obviously be very tentative and we cannot expect the computed surge amplitudes to be in too close agreement with the observations. The effects excluded in our theory might in some cases become significant. The surge may be amplified locally by the myriad of bays and fiords in these waters. In all three cases examined in

section 2, the observations indicate that this mechanism is important for the surges at Narvik. The topography of the continental shelf and the deep basin of the Norwegian sea may also have some influence on the surge amplitudes. A surge generated by a low pressure system while it is moving over the deep ocean west of the shelf, will be amplified when it propagates into the shallow water on the continental shelf. Particularly in Case I and Case III this effect might be important for the surge generation in the Lofoten region. For the wind generated part of the surge we expect that by including the deep ocean basin in our model, this would increase the speed of the free gravity waves and hence lead to a reduction of the computed surge amplitudes.

In order to apply our theory to the Cases I, II, and III as described in section 2, we have to estimate values of c_0 and f. We assume $c_0 =$ 50 m/s which corresponds to an average depth of 250 m and $f = 1.32 \times 10^{-4}\ s^{-1}$ corresponding to a latitude of 65° N. The parameters R, P, ν, and B can be estimated from the observations of the wind fields. The scaling factor for the surge amplitude, η_s, depends on the wind strength which usually varies when the south westerly wind fields propagate along the coast. Especially in Case I, and to some extent also in Case III, the wind speed increases while the wind propagates northward along the coast from Stad to Nordöyan and the wind direction changes from south to west when the pressure centers cross the coast line. Hence, to estimate values of η_s we have to estimate an average wind speed along the fetch distance. With the choosen values of c_0 and f, values of η_s for different wind speeds is given in Table 2.

Case I. Observations of the wind field lead to the rough estimates $P = 1$, $B = 1$, and $\nu = 0.5$. We also estimate the fetch to be $R = 1$ at Kristiansund and $R = 1.7$ at Rörvik. If we take into account the rather strong increase in wind speeds between Kristiansund and Rörvik, we find that the surge amplitudes are $\eta_{12} = 60$ cm at Kristiansund and $\eta_{12} = 120$ cm at Rörvik. These values are obtained from the surge diagrams in Fig. 9 and hence valid only for $B = 0$. Estimates of the surge amplitudes for $B = 1$ may be obtained from eq. (17), which show that these values have to be reduced by one half. When the low pressure center crosses the coast line, the wind field acting normal to the coast, intensifies and finally expands over the entire width of the shelf. This wind field has its maximum strength on the section of the coast between 64° N and 66° N. By using formula (18), we estimate $\eta_3 = 20$ cm at Kristiansund and $\eta_3 = 30$ cm at Rörvik. In this case and in Case III below, the low pressure center crosses the coast line in the Lofoten region. As a result the wind direction changes and be comes almost normal to coast. Hence the surge already generated by the south westerly wind field may interact with the surge generated by the wind component acting normal to the coast. Hence we estimate the maximum surge amplitude to be 50 cm at Kristiansund and 90 cm at Rörvik. The effect of a moving pressure field on sea level can be estimated from eq. (20). If we also take into account the decrease of the pressure westward from Kristiansund and Rörvik, we find that the pressure effect on sea level is hardly larger than the value obtained by considering the pressure field to be quasi static as suggested in section 2. (See Fig. 4.) Hence the estimate of the surge amplitude is in remarkable agreement with the recorded surge amplitude. This also applies to the time duration of the surge.

Case II. In this case the wind field extends far westward from the coast and the wind is almost parallel to it. Hence $B \cong 0$ and $T_{0y} \cong 0$. This time the cold front associated with the low pressure center, makes an oblique angle with the coast line. The wind field is therefore nearly stationary and we estimate P to be 0.5, and ν to be 0.2. The center of the wind field is situated approximately at 64° N. With a maximum wind speed of 30 m/s blowing for 12 hours, we obtain from eq. (17) a surge amplitude of 70 cm at this latitude. This amplitude is somewhat in excess of the observed surge amplitudes at Kristiansund and Rörvik. The reason for this discrepancy may be sought in the fact that our model does not include the deep ocean basin west of the shelf. In cases where the wind field extends west of the shelf (as in Case II), we expect our theory to overestimate the surge amplitudes.

Case III. The observations indicate that the values of P, B, and ν used in Case I are applicable. However, the wind component parallel to the coast along the section of the coast north of Kristiansund, is considerably less than in Case I. Accordingly we find that $\eta_{12} = 30$ cm at

Kristiansund, and $\eta_{12} = 40$ cm at Rörvik. In this case the wind component normal to the coast has its maximum strength further north than in Case I ($R \neq 0$), and we therefore estimate $\eta_3 = 10$ cm both at Kristiansund and at Rörvik. Hence the peak of the wind generated surge is about 40 cm at Kristiansund and 50 cm at Rörvik. By taking the effect of atmospheric pressure into account, it is again seen that the agreement with observations is remarkable.

These estimates of surge amplitudes demonstrate the importance of the various effects which contribute to large storm surges. The most favourable weather situation for generation of large amplitude storm surges is strong south westerly winds which blow along a large section of the coast. This usually occurs when a low pressure center moves relatively close to the coast and in a direction nearly parallel to it. In that case the surge may also be amplified considerably by atmospheric pressure variations. Case I and Case III are both examples to such situations.

If reliable forecasts of wind and pressure fields can be given, it should be possible to forecast large storm surges along the section of the Norwegian coast between 62° N and 68° N. It should also be possible to evaluate from the present theory rough estimates of the expected surge amplitudes.

Acknowledgements

The recordings of sea level have been made available to us by Norges Sjøkartverk and by Norges Geografiske Oppmåling. The wind data and the weather maps were provided by Norges Meteorologiske Institutt and Vervarslinga på Vestlandet. We acknowledge the kindness and the expediency our many requests to these institutions have been met with.

We also acknowledge the benefit of discussing this subject with Professor E. Jensen, University of Oslo. Mr S. Farstad, Romsdals Budstikke, Molde, brought the records of the catastrophic surge at Ona in 1670 to our attention.

REFERENCES

Abramowitz, M. & Stegun, I. A. 1964. *Handbook of mathematical functions*. National Bureau of Standards, Washington.

Bretschneider, C. 1967. Storm surges. *Advan. Hydrosci. 4*, 341–418.

Defant, A. 1961. *Physical oceanography*, vol. I, p. 420. Pergamon Press, New York.

Gammelsrød, T., Mork, M. & Røed, L. P. 1975. Upwelling possibilities at an ice edge. *Marine Science Communication Journal*. 1, 2, 115–145.

Heaps, N. S. 1965. Storm surges on a continental shelf. *Proc. Roy. Soc. A 257*, 351–383.

Helland, A. 1911. *Norges land og folk, Romsdals Amt*. Kristiania.

Johansen, S. 1959. On the effect of meteorological conditions upon the height of the sea level at the coast of southern Norway. *Met. Ann. 4*, no. 14. Det Norske Meteorologiske Institutt.

Miles, J. W. 1971. *Transforms in applied mathematics*. University Press, Cambridge.

Phillips, O. M. 1966. *The dynamics of the upper ocean*. University Press, Cambridge.

Welander, P. 1961. Numerical prediction of storm surges. *Advan. Geophys. 8*, 316–379.

ШТОРМОВЫЕ НАГОНЫ ВОДЫ ВДОЛЬ ЗАПАДНОГО ПОБЕРЕЖЬЯ НОРВЕГИИ

Изучаются ситуации штормовых нагонов воды вдоль западного побережья Норвегии между 62° и 68° с. ш. Наблюдения показывают, что большие нагоны вызываются сильными юго-западными ветрами, дующими вдоль большой части берега. Эта ситуация имеет место, когда интенсивный центр низкого давления движется относительно близко к берегу и почти параллельно ему. Изучается модель генерации нагона движущимся полем ветра, действующего вдоль прямолинейного берега. Получены и обсуждаются аналитические решения для амплитуды нагона вдоль берега. Теория применяется к ситуациям штормовых нагонов вдоль западного побережья Норвегии. Показано, что напряжение ветра в направлении вдоль берега и сила Кориолиса существенны для генерации больших нагонов. Компонента напряжения ветра, нормальная к берегу (т. е. северо-западные ветры) и изменения атмосферного давления дают меньший вклад в нагон.